Journal of Ceramic Processing Research. Vol. 2, No. 2, pp. 83~86 (2001)

JOURNAL OF
Ceramic Processing Research

Oxygen partial pressure dependence of the electrical conductivity of rare-earth-doped ceria ceramics

Soichiro Sameshima, Hiroko Wakita and Yoshihiro Hirata*
Department of Applied Chemistry and Chemical Engineering, Kagoshima University, 1-21-40 Korimoto, Kagoshima 890-0065, Japan

Rare-earth-doped ceria powders ($Ce_{0.8}R_{0.2}O_{1.9}$, R=Yb, Y, Gd, Sm, Nd and La), which may be applied to the oxygen ion electrolyte for solid oxide fuel cells, were prepared by the oxalate coprecipitation method. As-produced powders were calcined at 600°C, then pressed isostatically into disks (8 mm in diameter and 1 mm thickness) and sintered to above 98% relative density at 1600°C for 4 h. The complex impedance of the disk samples with Au electrodes was measured by a two-terminal AC bridge circuit in an oxygen partial pressure range from 0.21 to 1×10^{-23} atm at 336°-866°C. The electrical conductivity of Yb, Y or Sm-doped ceria was independent of the oxygen partial pressure. This result indicates that the conductivity is dominated by the diffusion of oxygen ions and electronic conduction can be ignored in the present case.

Key words: Rare-earth-doped ceria, Electrical conductivity, Oxygen partial pressure.

Introduction

The established solid oxide fuel cell (SOFC) consists of yttria-stabilized zirconia (YSZ) electrolyte, Ni/YSZ cermet anode, $La_{1-x}Sr_xMnO_3$ cathode, and $LaCrO_3$ inter-connecter [1]. This system is operated at about 1000°C to increase the diffusion rate of oxygen ions. However, reducing the operation temperature leads to an increase of lifetime and the expansion of choice of the constituent materials such as electrodes and metal gas separator of the SOFC. It is reported that rare-earth-doped ceria (RDC) has a higher oxygen ion conductivity than YSZ and is a candidate solid electrolyte for the low temperature operation of SOFC [2-7]. The serious problem reported is the increase of electronic conduction caused by the reduction of Ce^{4+} to Ce^{3+} at lower oxygen pressure. Some researchers attempted to suppress the electronic conduction by the addition of Pr_6O_{17} [8], alkali-element or Ca to RDC [9, 10], or by coating RDC with YSZ [11]. The oxygen partial pressure range for no significant electronic conduction was expanded from 10^{-8} atm for $Ce_{0.75}Sm_{0.25}O_{1.88}$ to 10^{-10} atm for $(Sm_{0.5}Ca_{0.5})_{0.225}Ce_{0.775}O_{1.86}$ or to 10^{-14} atm for $(Sm_{0.936}Cs_{0.06}Li_{0.04})_{0.25}Ce_{0.75}O_{1.86}$ [10]. It is reported that the coating by a YSZ thin film on the anode side of the solid electrolyte was effective in suppressing the reduction of $Ce_{0.8}R_{0.2}O_{1.9}$. This paper reports the dependence of electrical conductivity of RDC on oxygen partial pressure and discusses the electronic conduction.

*Corresponding author:
Tel : +81-99-285-8325
Fax: +81-99-257-4742
E-mail: hirata@apc.kagoshima-u.ac.jp

Experimental Procedure

RDC powders ($Ce_{0.8}R_{0.2}O_{1.9}$, R=Yb, Y, Gd, Sm, Nd, La) were prepared by calcining oxalate coprecipitate at 600°C in air [12, 13]. As-calcined powders consisted of submicrometre-sized particles of 0.5-1 μm in length and were compacted isostatically under a pressure of 294 MPa to a pellet of 10 mm in diameter and 2 mm in thickness. The sintering at 1600°C for 4 h gave dense compacts above 98% of theoretical density. Gold was sputtered on the RDC polished with diamond paste of 0.25 μm. Gold paste (TR-1301, Tanaka Kikinzoku Kogyo Co., Japan) was spread homogeneously on the Au electrodes and heated to 940°C in air. Platinum plates with Pt lead wires were pressurized to contact the Au electrodes. The complex impedance of the sample in the temperature range of 300° to 800°C, was measured by a two-terminal AC bridge circuit using a self-inductance-capacitance-impedance (LCZ) meter (model 4276A, 4277A and 4193A, Yokogawa Hewlett-Packard Co., Tokyo, Japan) at 100 Hz to 110 MHz. The conductivity of samples was corrected with the resistance of the measurement apparatus. The oxygen partial pressure was controlled in the atmosphere of the H_2-H_2O system and was monitored with an YSZ oxygen sensor (KOA-200, Kaken Inc., Ibaraki, Japan).

Results

Electrical properties of RDC in air

Figure 1 shows the impedance plot of $Ce_{0.8}Y_{0.2}O_{1.9}$ at 336°C. The impedance plot was divided into two skewed semicircles on the Z'-axis (real part). The smaller semicircle in the higher frequency range and the larger

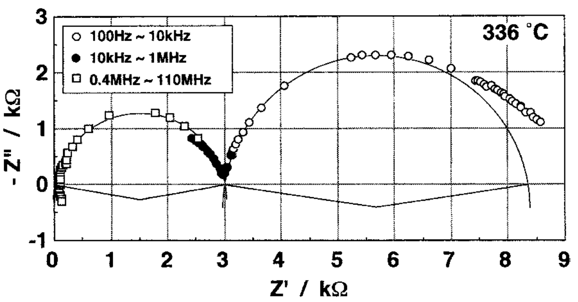

Fig. 1. Impedance diagram of $Ce_{0.8}Y_{0.2}O_{1.9}$ at 336 °C in air.

semicircle in the lower frequency range may correspond to oxygen ion migration in the bulk and across grain boundaries, respectively [14]. The bulk and grain boundary resistance of samples was determined from the Z' values at Z" = 0. Figure 2 shows the impedance plots of $Ce_{0.8}Y_{0.2}O_{1.9}$ at 536° and 630°C. The impedance plot at 536°C consisted of a straight line with a slope close to $\pi/4$ in the lower frequency range, a semicircle in the intermediate frequency range and a vertical line parallel to the Z" axis in the higher frequency range. The semicircle disappeared at 630°C. The possible equivalent circuits are shown in Fig. 2(c) and (d). The sample resistance corresponds to $(R_1 + R_2)$ and R at 536° and 630°C, respectively. The straight line in the lower frequency range is associated with the diffusion of oxygen ions towards or from the electrode/ electrolyte interface (Warburg impedance, $Z_w = k\ (1-j)/\sqrt{\omega}$, k: constant, $\omega = 2\pi f$, f: frequency). The vertical line in the higher frequency range reflects the coil component of the lead wire. The bulk resistance and sample resistance $(R_1 + R_2)$ were converted to conductivity using the thickness of the sample and surface area of electrodes. Figure 3 shows the Arrhenius plots of electrical conductivity for $Ce_{0.8}Y_{0.2}O_{1.9}$ in the oxygen partial pressure range from 0.21 to 1×10^{-23} atm. The activation energies in air were 85.2 and 99.0 kJ/mol for the bulk conductivity and total conductivity, respectively. These values were close to the reported activation energies (86.5 kJ/mol for bulk conductivity and 89.7 kJ/mol for total conductivity) [14].

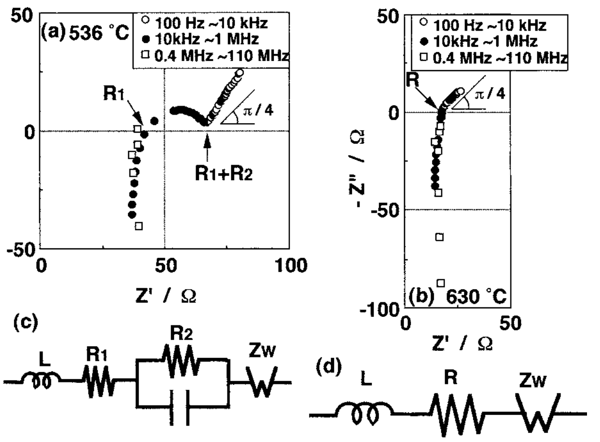

Fig. 2. Impedance diagrams for $Ce_{0.8}Y_{0.2}O_{1.9}$ at (a) 536° and (b) 630°C in air and corresponding equivalent circuits (c, d).

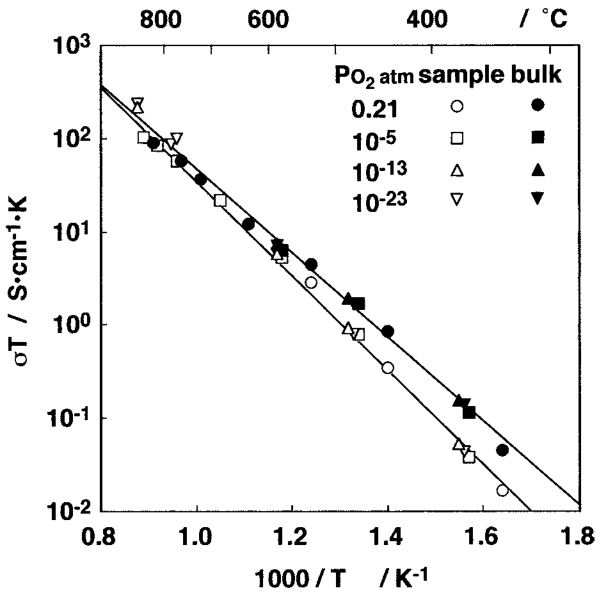

Fig. 3. Arrhenius plots of bulk conductivity and sample conductivity of RDC in the oxygen partial pressure range from 0.21 to 10^{-23} atm. Sample conductivity was determined from the total of bulk resistance and grain boundary resistance.

Electrical properties of RDC in low oxygen partial pressure

Figure 4 shows the impedance diagrams for $Ce_{0.8}Y_{0.2}O_{1.9}$ at 359-366°C in oxygen pressures of 10^{-13} and 10^{-23} atm. The impedance plots were similar to those measured in air. That is, the interpretation of the measured result is the same as mentioned before. The

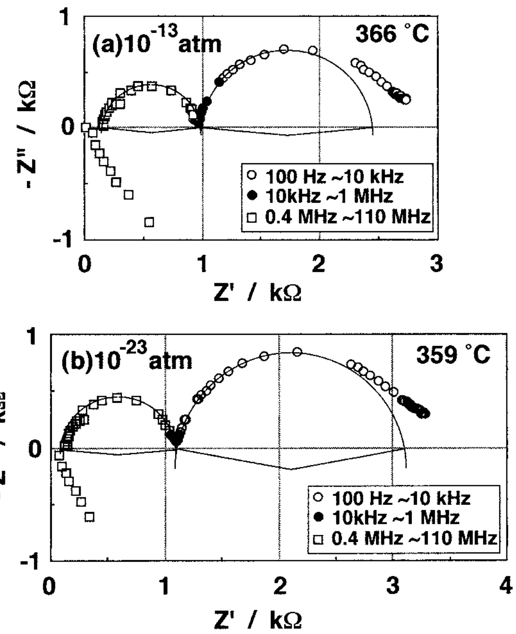

Fig. 4. Impedance diagrams for $Ce_{0.8}Y_{0.2}O_{1.9}$ at 359-366°C in the oxygen pressure of (a) 1×10^{-13} and (b) 1×10^{-23} atm.

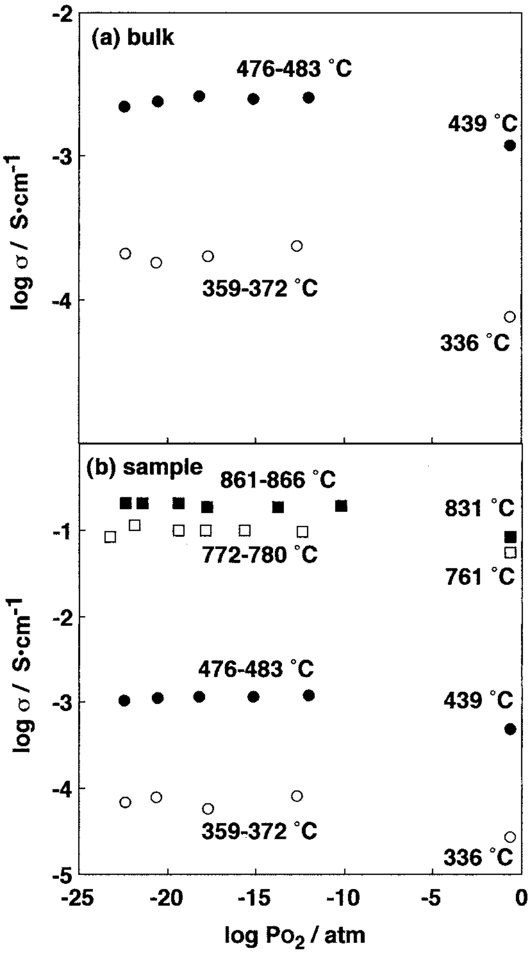

Fig. 5. Bulk (a) and sample (b) conductivities of $Ce_{0.8}Y_{0.2}O_{1.9}$ as a function of oxygen partial pressure.

Z" values in the higher frequency range are associated with the inductance (L) of the measurement lead wire. The misfit of Z' value near the origin in the high frequency range is under investigation. Figure 5 shows the electrical conductivity of $Ce_{0.8}Y_{0.2}O_{1.9}$ as a function of oxygen partial pressure in the temperature range from 336° to 866°C. The sample conductivity was not sensitive to the oxygen partial pressure in the range from 0.21 to 10^{-23} atm. Similarly little dependency of bulk conductivity on oxygen partial pressure was measured. Figure 3 shows the Arrhenius plots of electrical

Table 1. Activation energy of the bulk and sample conductivity for $Ce_{0.8}Y_{0.2}O_{1.9}$

Oxygen partial pressure atm	Activation Energy kJ/mol	
	bulk	sample
0.21 [14]	86.5	89.7
0.21	85.2	99.0
1×10^{-5}	86.3	96.7
1×10^{-13}	84.5	104.4
1×10^{-23}	84.4	104.4

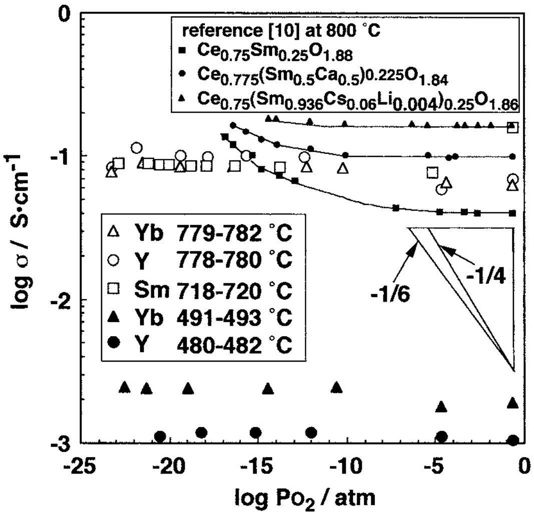

Fig. 6. Effect of dopant on the sample conductivity of $Ce_{0.8}R_{0.2}O_{1.9}$ (R=Yb, Y, Sm).

conductivity for $Ce_{0.8}Y_{0.2}O_{1.9}$ in the lower oxygen partial pressure range. Table 1 summarizes the activation energy of electrical conductivity for $Ce_{0.8}Y_{0.2}O_{1.9}$. The bulk conductivity and its activation energy were independent of the oxygen partial pressure. As seen in Fig. 3, the sample conductivity and its activation energy were also close over the wide oxygen pressure range. Figure 6 shows the effect of dopant on the conductivity of RDC (R=Yb, Y and Sm). The conductivities at 0.21 and 1×10^{-5} atm oxygen pressure were estimated from the data in Fig. 3 to compare at a similar temperature. All the samples showed a small dependency of conductivity on the oxygen partial pressure.

Discussion

The formation of the electrons in RDC is expressed by Eq. (1),

$$O_O^{\times} \xrightleftharpoons{K_1} V_O^{\bullet\bullet} + 2\,e' + \frac{1}{2}O_2(g) \tag{1}$$

The equilibrium constant K_1 is expressed by Eq. (2) because $[O_O^{\times}]$ can be approximated to be 1.

$$K_1 = P_{O_2}^{1/2}[V_O^{\bullet\bullet}][e']^2 \tag{2}$$

The substitution of a rare-earth-element for Ce in the CeO_2 fluorite structure produces an oxygen vacancy as expressed by Eq. (3),

$$R_2O_3 \xrightarrow{CeO_2} 2R_{Ce}' + 3O_O^{\times} + V_O^{\bullet\bullet} \tag{3}$$

That is, the concentration of oxygen vacancies is a total given by Eqs. (1) and (3),

$$[V_O^{\bullet\bullet}] = \frac{1}{2}[R_{Ce}'] + \frac{1}{2}[e'] \quad (4)$$

When the concentration of oxygen vacancies is dominated by Eq. (3), the following relation is derived,

$$[V_O^{\bullet\bullet}] = \frac{1}{2}[R_{Ce}'] \quad (5)$$

Substitution of Eq. (5) into Eq. (2) yields Eq. (6),

$$[e'] = (2K_1)^{1/2}[Y_{Ce}']^{-1/2}P_{O_2}^{-1/4} \quad (6)$$

Equation (6) indicates a linear relation of a log [e']-log P_{O_2} plot with a slope of −1/4. On the other hand, when Eq. (1) is independent of Eq. (3), the following relation is derived from Eq. (1),

$$[V_O^{\bullet\bullet}] = \frac{1}{2}[e'] \quad (7)$$

A combination of Eqs. (2) and (7) gives the following equation,

$$[e'] = (2K_1)^{1/3}P_{O_2}^{-1/6} \quad (8)$$

Equation (8) indicates a slop of −1/6 for a log [e']-log P_{O_2} plot. As seen in Figs. 5 and 6, the electrical conductivity of RDC was independent of the oxygen partial pressure from 0.21 to 10^{-23} atm, suggesting a low electronic conduction. The electrical conductivity of RDC measured by Mori *et al*. [10] is shown in Fig. 6. Their data increased in the lower oxygen partial pressure range below 10^{-8} atm at 800°C because of the reduction of CeO_2. Their slops of log σ - log P_{O_2} plot were −0.10 to −0.19, and close to the theoretical values, −1/6, as shown in Eq. (8). In this experiment, all the X-ray diffraction peaks for $Ce_{0.8}Y_{0.2}O_{1.9}$ after the impedance measurement in the low oxygen partial pressure were assigned to a cubic solid solution of CeO_2. No peak of Ce_2O_3 was detected, suggesting little reduction of Ce^{4+} to Ce^{3+}. The discrepancy of the data between Mori *et al*. and this experiment suggests that the electrical properties of RDC are significantly sensitive to the processing used. According to Xiong *et al*. [15], the electrical conductivity of the ZrO_2-CeO_2-Y_2O_3 system at 1000°C is proportional to −1/4th power of the oxygen pressure, indicating electronic conduction associated with a reduction of Ce^{4+} to Ce^{3+} ($2CeO_2 \rightleftarrows Ce_2O_3 + V_O^{\bullet\bullet} + 2e' + 1/2O_2$). The result obtained in this experiment concludes that the two component systems of RDC are more stable than the three component system of ZrO_2-CeO_2-Y_2O_3 at a lower oxygen potential pressure.

Conclusions

The electrical conductivity of $Ce_{0.8}R_{0.2}O_{1.9}$ (R=Yb, Y, Sm) was independent of the oxygen partial pressure in the range from 0.21 to 10^{-23} atm at 336°-866°C, suggesting a low electronic conduction and high oxygen ion conduction. The activation energy was 85.2 kJ/mol for the migration of oxygen ions in the bulk of Y-doped ceria.

References

1. K. Eguchi, J. Alloys and Compounds, 250 (1997) 486-491.
2. T. H. Etsell and S. N. Flengas, Chem. Rev. 70[3] (1970) 339-376.
3. T. Kudo and H. Obayashi, J. Electrochem. Soc. 122[1] (1975) 142-147.
4. H. L. Tuller and A. S. Nowick, J. Electrochem. Soc. 122[2] (1975) 255-259.
5. R. T. Dirstine, R. N. Blumenthal and T. F. Kuech, J. Electrochem. Soc. 126[2] (1979) 264-269.
6. B. C. H. Steele, K. Zheg, R. A. Rudkin, N. Kiratzis and M. Christie, in Proceedings of the Fourth International Symposium on Solid Oxide Fuel Cells (SOFC-IV), June 1995, edited by M. Dokiya, O. Yamamoto, H. Tagawa and S. C. Singhal (The Electrochem. Soc., Inc., New Jersey, 1995) pp.1028-1038.
7. H. Inaba and H. Tagawa, Solid State Ionics, 83 (1996) 1-16.
8. D. L. Maricle, T. E. Swarr and S. Karavolis, Solid State Ionics 52 (1992) 173-182.
9. T. Mori and H. Yamamura, J. Am. Ceram. Soc. 79[12] (1996) 3309-3312.
10. T. Mori, T. Ikegami and H. Yamamura, J. Electrochem. Soc. 146[12] (1999) 4380-4385.
11. T. Inoue, T. Setoguchi, K. Eguchi and H. Arai, Soild State Ionics 35 (1989) 285-291.
12. K. Higashi, K. Sonoda, H. Ono, S. Sameshima and Y. Hirata, Key Eng. Mater. 159-160 (1999) 25-30.
13. K. Higashi, K. Sonoda, H. Ono, S. Sameshima and Y. Hirata, J. Mater. Res. 14[3] (1999) 957-967.
14. S. Sameshima, H. Ono, K. Higashi, K. Sonoda, Y. Hirata and Y. Ikuma, J. Ceram. Soc. Jpn. 108[12] (2000) 1060-1066.
15. Y. Xiong, K. Yamaji, N. Sakai, H. Negishi, T. Horita and H. Yokokawa, in Proceedings of the Seventh International Symposium on Solid Oxide Fuel Cells (SOFC-VII), 2001, in press.